J. Fluid Mech. (2006), *vol.* 546, *pp.* 89–111.
doi:10.1017/S0022112005007020 Printed in the United Kingdom

Localized mode of sound in a waveguide with Helmholtz resonators

By N. SUGIMOTO AND H. IMAHORI

Division of Nonlinear Mechanics, Department of Mechanical Science, Graduate School of Engineering Science, University of Osaka, Toyonaka, Osaka 560-8531, Japan

(Received 12 July 2004 and in revised form 22 June 2005)

This paper examines the existence of a localized mode of sound in a planar waveguide between two parallel rigid walls with a pair of identical Helmholtz resonators connected to the upper and lower walls. The localized mode means that linear free oscillations at a particular frequency are trapped only in the vicinity of the resonators and decay exponentially away from them. Assuming the waveguide extends infinitely, a two-dimensional problem is solved fully within lossless theory. It is revealed that, in a waveguide with the resonators connected exactly opposite to each other, the localized mode can exist at a frequency lower than the lowest cutoff frequency of the waveguide and the natural frequency of the resonator. Then the pressure field is antisymmetric spanwise with respect to the centreline of the waveguide, and symmetric axially with respect to the resonators. The localized mode is represented by the superposition of an infinite number of anti-symmetric evanescent modes and no plane-wave mode is involved. The absence of the latter mode makes it possible to localize sound without it being accompanied by radiation damping. This explains why no symmetric localized mode over the width exists. In a waveguide with the resonators offset, no localized mode is shown to exist generally except for a particular spacing. Generalization to cases with multiple pairs of resonators is also considered.

1. Introduction

A tube with an array of Helmholtz resonators has been used to demonstrate the generation of an acoustic solitary wave in air (Sugimoto *et al.* 2004). In designing the tube for experiments, the problem has arisen of how the resonators should be distributed on the tube. After much consideration, they are connected in a staggered configuration on both sides of the circular tube rather than facing each other. One reason of this choice is because localized oscillations around the resonators might be expected, and they might give rise to unfavourable effects on the propagation of the acoustic solitary wave which would obscure its observation. Motivated by clarifying this problem, the present paper examines the existence of the localized mode of sound by considering a two-dimensional configuration for the sake of mathematical simplicity.

In the present context, the localized mode is taken to mean linear and free oscillations at a particular frequency trapped only in the vicinity of the resonators and accompanied by no radiation into infinity. The existence of such a trapped wave or mode was unveiled long ago in seminal paper by Ursell (1951) in a deep water-wave channel with a submerged thin cylinder, and later proven by Jones (1953) and Ursell (1987) for a wide class of submerged cylinders. A few decades later, it

has attracted much attention and has been investigated intensively by Evans, McIver, Linton and others cited below not only for water-wave channels but also for acoustic and electromagnetic waveguides as well as elastic beams. Although water waves appear different physically from acoustic and electromagnetic waves, the analysis uses the same Helmholtz equation if the time and depth dependence is removed. For flexural waves on beams, on the other hand, the wave equation is the Bernoulli–Euler equation of fourth order (Abramian, Andreyev & Indejtchev 1995).

In the context of acoustics, Evans & McIver (1991), Evans & Linton (1991), Callan, Linton & Evans (1991), Evans (1992) and Evans, Levitin & Vassiliev (1994) showed that if a symmetric body is placed symmetrically in a two-dimensional waveguide with parallel rigid walls, i.e. a body with a rectangular cross-section or a circular cylinder is placed on the centreline of the waveguide with its axis normal to the centreline, then the trapped mode is possible at a frequency lower than the lowest cutoff frequency of the waveguide modes and then the pressure field is anti-symmetric spanwise with respect to the centreline but symmetric axially with respect to the body. Mathematically the existence of such a discrete frequency corresponds to a point isolated spectrum, in addition to ordinary continuous ones, of the Laplacian operator in an unbounded domain, usually with Neumann boundary conditions. If such a trapped mode exists, the radiation condition at infinity is not able to single out the solution in scattering problems so that uniqueness of solution is lost.

After the pioneering work above, many papers have been published that examine the existence or otherwise of the trapped mode in cases where: (i) symmetry in configuration of body or its position in the waveguide is broken (Evans, Linton & Ursell 1993; Linton *et al.* 2002), (ii) the waveguide is deformed locally to include an indentation, i.e. a cavity without a throat (Evans & Linton 1991; Evans *et al.* 1994; Koch 2004) or to include grooves in the context of microwaves (Fernyhough & Evans 1998), (iii) the two-dimensional waveguide and body are replaced by a circular tube with a sphere (Ursell 1991) or with a cylinder (Linton & McIver 1998), (iv) rigid walls with Neumann boundary conditions are replaced by soft walls with Dirichlet boundary conditions (McIver & Linton 1995), and (v) multiple bodies or a periodic array of bodies are placed in the waveguide (Evans & Porter 1997; Porter & Evans 1999). It is shown that there may occur a case where the frequency is located above the cutoff frequency and embedded in a continuous spectrum (Evans & Porter 1998; McIver *et al.* 2001; Koch 2004). In any case, it seems to be common for trapped modes to be found in theory, though dependent crucially on geometry. Up to the present, however, there is little experimental evidence to support the existence of these localized oscillations. However, Parker & Stoneman (1989) describe experiments on acoustic resonance due to trapped modes about a solid body placed in a duct flow and Woodley & Peake (1999*a*, *b*) describe some applicable to acoustic resonance in turbomachinery.

A waveguide with Helmholtz resonators connected provides a new situation not considered so far. While an indentation may be compared with a so-called quarter-wavelength tube, the Helmholtz resonator with a throat is different and may be treated simply. It will be shown that full solutions are available easily so that the frequency of localized oscillations is obtained as a root of an algebraic frequency equation. Before embarking on an analysis, some preliminary discussions are given in § 2 on sound propagation in a planar waveguide and radiation damping when a single resonator is connected. A waveguide with a pair of resonators is analysed in § 3 by applying the method of Fourier transform. The sound field is presented explicitly in closed form, and frequency equations are derived for the anti-symmetric and symmetric modes, respectively. Then, by seeking roots to the frequency equation, the localized oscillations

are shown to occur only for the anti-symmetric mode at a frequency below the lowest cutoff frequency and the natural frequency of the resonator. In § 4, discussions are given on the non-existence of localized oscillations in the symmetric mode and also on those in a tube when the resonators are offset. In § 5, the localized mode in the waveguide with multiple pairs of resonators connected is also considered. After describing the case of two pairs in detail, generalization to $N(\geqslant 3)$ identical pairs is briefly discussed.

2. Preliminaries

This section is devoted to preliminaries to the analyses in following sections. Note that all dissipative effects are neglected.

2.1. *Propagating and evanescent modes in a waveguide*

Sound propagation is governed by the following wave equation:

$$\frac{\partial^2 \phi}{\partial t^2} = a_0^2 \left(\frac{\partial^2 \phi}{\partial x^2} + \frac{\partial^2 \phi}{\partial y^2} \right), \tag{2.1}$$

with

$$p' = -\rho_0 \frac{\partial \phi}{\partial t}, \tag{2.2}$$

where $\phi(x, y, t)$ and $p'(x, y, t)$ denote, respectively, the velocity potential and the excess pressure over the equilibrium (atmospheric) one p_0, while a_0 and ρ_0 denote, respectively, the sound speed and the density of air in equilibrium, t being the time and (x, y) the in-plane coordinates of the two-dimensional waveguide. Taking the x-axis along the waveguide and the y-axis perpendicular to it, the origin is chosen at a midpoint of the two waveguide walls. Assuming the walls to be parallel and rigid, the boundary conditions require that

$$\frac{\partial \phi}{\partial y} = 0 \quad \text{at} \quad y = \pm \frac{H}{2}, \tag{2.3}$$

where H denotes the waveguide width.

When the waveguide is unbounded in the x-direction, an elementary solution to (2.1) is

$$\phi = C \cos \left[m\pi \left(\frac{y}{H} + \frac{1}{2} \right) \right] \exp[\mathrm{i}(kx - \omega t)] + \text{c.c.}, \tag{2.4}$$

C being an arbitrary constant and c.c. denoting complex conjugate of the preceding term. A dispersion relation between a wavenumber k and an angular frequency ω must be satisfied, which is given by

$$\omega^2 = \frac{a_0^2}{H^2} [(m\pi)^2 + (kH)^2], \tag{2.5}$$

where m is an integer ($m = 0, 1, 2, \ldots$) and accounts for an infinite number of modes.

Figure 1 shows the dispersion relation, where the abscissa shows the magnitude of the dimensionless wavenumber $|kH|$ and the ordinate the dimensionless angular frequency $\omega H/a_0$. The solid lines designate propagating modes. The straight line with $m = 0$ represents the lowest non-dispersive mode while the curved lines represent dispersive modes with cutoff frequencies $H\omega/a_0 = m\pi$ at $kH = 0$. Below the frequencies, kH becomes purely imaginary, and these are evanescent modes. In figure 1, they are drawn as broken lines. Localized oscillations to be sought occur typically at an angular frequency below the lowest cutoff frequency $\omega H/a_0 = \pi$, the

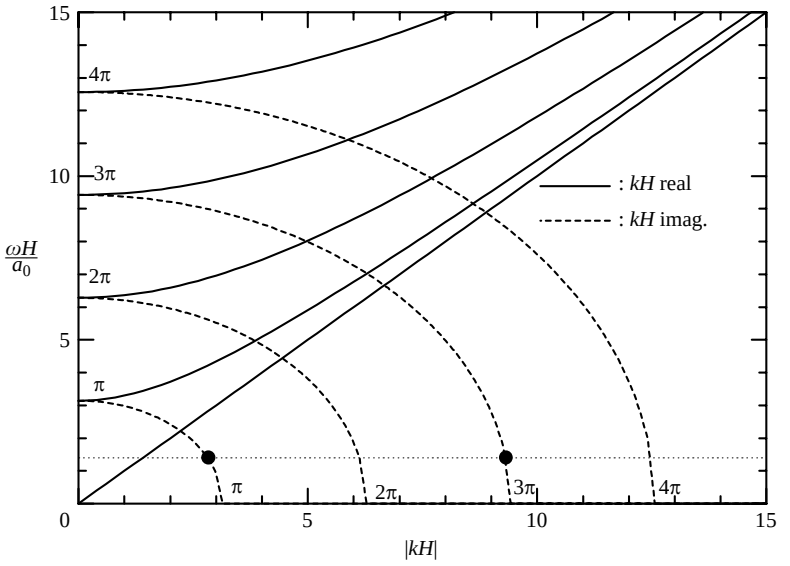

FIGURE 1. Dispersion relation for sound in a two-dimensional waveguide of width H where kH and $\omega H/a_0$ denote, respectively, the dimensionless wavenumber and frequency, and the solid and broken lines represent, respectively, the propagating modes with real value of kH and the evanescent modes with pure imaginary value of kH, and the dotted horizontal line represents a frequency of localized oscillations below the cutoff frequency at $\omega H/a_0 = \pi$, the solid circles indicating anti-symmetric modes involved.

dotted horizontal line and the solid circles representing, respectively, the frequency and anti-symmetric modes involved.

From the form of the eigenfunctions, the mode with $m = 0$ corresponds to a plane wave. Note that each eigenfunction becomes an even or odd function of y according to whether m is even or odd, respectively, and that the following relations hold:

$$\int_{-H/2}^{H/2} \cos\left[m\pi\left(\frac{y}{H}+\frac{1}{2}\right)\right] \mathrm{d}y = 0, \tag{2.6}$$

except for the mode with $m = 0$. These relations imply that the velocity in the x-direction and excess pressure averaged over the width of the waveguide exist only for the plane-wave mode and vanish otherwise.

2.2. *Response of a Helmholtz resonator and its acoustic admittance*

The theory for the response of a Helmholtz resonator is summarized briefly (Sugimoto 1992). Figure 2 shows a waveguide with a single resonator connected in the two-dimensional configuration. The resonator consists of a cavity of area S, and of a throat of length L having uniform width B. Ignoring the motion of air in the cavity and the compressibility of air in the throat, the conservation of mass in the cavity and the momentum balance in the throat require that

$$S\frac{\mathrm{d}\rho_\mathrm{c}}{\mathrm{d}t} = \rho_0 B w \quad \text{and} \quad \rho_0 L\frac{\mathrm{d}w}{\mathrm{d}t} = p'_\mathrm{t} - p'_\mathrm{c}, \tag{2.7}$$

where ρ_c and p'_c denote, respectively, the mean density of air in the cavity and the mean excess pressure therein, while w and p'_t denote, respectively, the velocity of air going into the throat and the excess pressure at the orifice of the throat, which

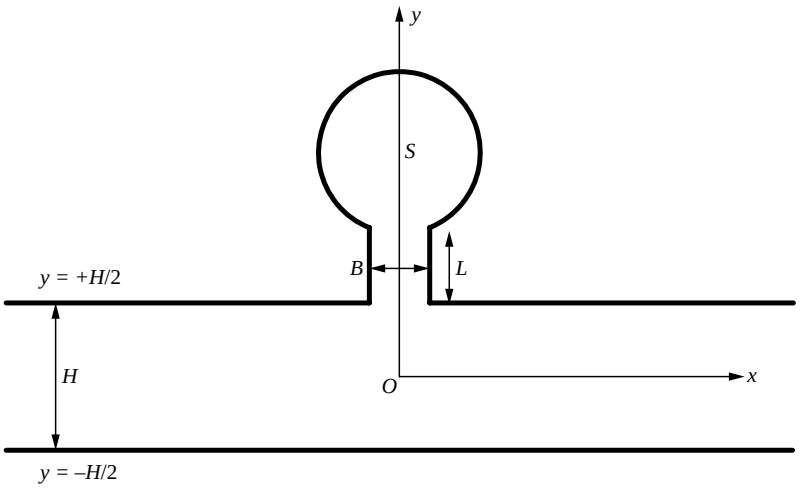

FIGURE 2. A waveguide with a single Helmholtz resonator connected in the two-dimensional configuration.

are assumed to be uniform over the width of the throat. In addition, w is regarded as being uniform along the throat because its length is much shorter than a typical wavelength of sound.

Assuming the adiabatic change for air in the cavity ($\mathrm{d}p'_\mathrm{c}/\mathrm{d}\rho_\mathrm{c} = a_0^2$), elimination of w from (2.7) yields

$$\frac{\mathrm{d}^2 p'_\mathrm{c}}{\mathrm{d}t^2} + \omega_0^2 p'_\mathrm{c} = \omega_0^2 p'_\mathrm{t}, \tag{2.8}$$

where ω_0 ($= \sqrt{a_0^2 B/LS}$) is a natural angular frequency of the resonator. As a common practice, L is lengthened by making so-called end corrections to find better agreement with experiments. But we do not go into the details here (see Sugimoto *et al.* 2004).

Next we consider a 'steady state' where p'_t oscillates harmonically at an angular frequency ω, and p'_c and w follow it in the form:

$$\begin{bmatrix} p'_\mathrm{t} \\ p'_\mathrm{c} \\ w \end{bmatrix} = \begin{bmatrix} P_\mathrm{t} \\ P_\mathrm{c} \\ W \end{bmatrix} \exp(\mathrm{i}\omega t) + \text{c.c.}, \tag{2.9}$$

where P_t, P_c, and W are respective complex amplitudes of oscillations. The acoustic admittance Y of the resonator is defined by the ratio of the 'volume' flux BW to P_t as

$$Y \equiv \frac{BW}{P_t} = \frac{B}{\rho_0 L}\left(\frac{\mathrm{i}\omega}{\omega_0^2 - \omega^2}\right). \tag{2.10}$$

With all lossy effects ignored, Y is purely imaginary, and diverges at the natural angular frequency, beyond which the phase jumps from $\pi/2$ to $-\pi/2$.

2.3. *Radiation damping and non-existence of free oscillations*

We now consider propagation in the waveguide with a single resonator connected at $x = 0$ as shown in figure 2. Supposing that the width of the throat is narrow enough in comparison with the waveguide width, the resonator is regarded as being connected at the point $x = 0$, for simplicity.

If the resonator were to oscillate at an angular frequency ω, then sound would be radiated into the waveguide in both directions of x. This process is accompanied by some net flow of mass over the width of the waveguide, though oscillatory in time. In view of (2.6), it is natural to assume that the excess pressure p' and the axial velocity u $(= \partial\phi/\partial x)$ in the waveguide are given in the plane-wave mode as follows:

$$p' = \begin{cases} +\rho_0 a_0 u = f(t - x/a_0) & \text{for } x > 0, \\ -\rho_0 a_0 u = f(t + x/a_0) & \text{for } x < 0, \end{cases} \tag{2.11}$$

where $\rho_0 a_0$ is the acoustic impedance, $f(t)$ is an unknown function to be determined by matching conditions at the junction, and no incoming waves to the resonators are assumed.

At $x = 0$, the conditions require continuity of mass flux and pressure, which are given, respectively, as follows:

$$Bw = -\frac{2Hf(t)}{\rho_0 a_0} \quad \text{and} \quad p'_{\mathrm{t}} = p' = f(t). \tag{2.12}$$

Using $Bw = (S/\rho_0 a_0^2)\,\mathrm{d}p'_{\mathrm{c}}/\mathrm{d}t$ from the first equation of (2.7), it follows from (2.12) that $f(t) = -(S/2a_0H)\,\mathrm{d}p'_{\mathrm{c}}/\mathrm{d}t$. Substituting this into the right-hand side of (2.8), we derive

$$\frac{\mathrm{d}^2 p'_c}{\mathrm{d}t^2} + \mu\frac{\mathrm{d}p'_c}{\mathrm{d}t} + \omega_0^2 p'_c = 0, \tag{2.13}$$

with $\mu = a_0 B/2HL$. The appearance of the second term suggests that no free oscillations persist. In fact, p'_{c} is given by $\exp(\mathrm{i}\omega t)$ with a complex angular frequency

$$\omega = \omega_0 + \mathrm{i}\frac{a_0 B}{4HL} + O\left(\mu^2/\omega_0^2\right), \tag{2.14}$$

for $\mu/\omega_0 = (B/2H)(a_0/\omega_0 L) \ll 1$. Although $a_0/\omega_0 L$, the ratio of a typical wavelength to the throat length, is large, μ/ω_0 is small because $B/H \ll 1$. For example, when $B/H = 0.1$, $\omega_0/2\pi = 240$ Hz and $L = 0.04$ m, $\mu/\omega_0 \approx 0.28$. In spite of the fact that no dissipative effects are included, no oscillations persist. This is because the energy contained in the resonator is carried out by radiation to infinity, which is known as radiation damping.

3. Localized mode in a waveguide with a pair of Helmholtz resonators

3.1. *Formulation of the problem*

We now consider a waveguide with a pair of identical Helmholtz resonators connected exactly opposite to each other in the upper and lower walls as shown in figure 3. In the preceding section, the resonator was regarded as being connected at the point $x = 0$ on assuming that the width is narrow. Here the width is allowed to be finite and the boundary conditions at the wall are imposed as follows:

$$\frac{\partial\phi}{\partial y} = \pm w^{\pm} \quad \text{for} \quad |x| < B/2 \quad \text{at} \quad y = \pm H/2, \tag{3.1}$$

and otherwise $\partial\phi/\partial y = 0$ at $y = \pm H/2$ where $w^{\pm}$ is taken positive for flows directed from the waveguide into the respective resonators. Here and hereafter the sign '$\pm$' (and '$\mp$' to be used later) which appears simultaneously is taken to be vertically ordered.

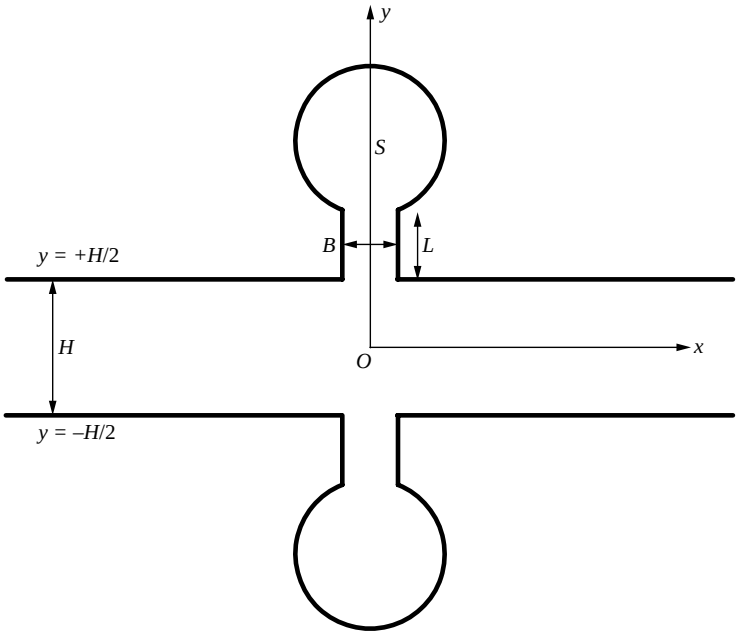

FIGURE 3. A waveguide with a pair of identical Helmholtz resonators connected exactly opposite to each other in the upper and lower walls in the two-dimensional configuration.

We look for solutions of harmonic oscillations at an angular frequency ω (> 0) by setting

$$\begin{bmatrix} \phi \\ p' \\ p'^{\pm}_{c} \\ w^{\pm} \end{bmatrix} = \begin{bmatrix} \Phi(x, y) \\ P(x, y) \\ P^{\pm}_{c} \\ W^{\pm} \end{bmatrix} \exp(\mathrm{i}\omega t) + \text{c.c.} \tag{3.2}$$

Then Φ satisfies the Helmholtz equation:

$$\frac{\partial^2 \Phi}{\partial x^2} + \frac{\partial^2 \Phi}{\partial y^2} + k^2 \Phi = 0 \quad \text{in} \quad -\infty < x < \infty \quad \text{and} -H/2 < y < H/2, \tag{3.3}$$

with $k^2 = \omega^2/a_0^2$. Since the throat width is so small that variations over the width may be ignored, it is assumed that the complex 'volume' fluxes $BW^{\pm}$ are given by the complex pressure P at the centre of the width as follows:

$$BW^{\pm} = Y P(x = 0, y = \pm H/2). \tag{3.4}$$

Rewriting the boundary conditions (3.1) in terms of (3.2), $W^{\pm}$ is decomposed into the anti-symmetric component W^a and symmetric one W^s as follows:

$$\frac{\partial \Phi}{\partial y} = \begin{cases} +W^+ = W^a + W^s & \text{for } |x| < B/2 \text{ at } y = +H/2, \\ -W^- = W^a - W^s & \text{for } |x| < B/2 \text{ at } y = -H/2, \end{cases} \tag{3.5}$$

with

$$W^a = \tfrac{1}{2}(W^+ - W^-) \quad \text{and} \quad W^s = \tfrac{1}{2}(W^+ + W^-). \tag{3.6}$$

By this decomposition, Φ may be sought as the sum of the anti-symmetric component Φ^a and the symmetric one Φ^s, which are odd and even functions of y, respectively.

3.2. *Solution by the method of Fourier transform*

The anti-symmetric solution Φ^a is first sought by using the method of Fourier transform defined as

$$\hat{\Phi}^a(k, y) \equiv \frac{1}{\sqrt{2\pi}} \int_{-\infty}^{\infty} \Phi^a(x, y) \mathrm{e}^{\mathrm{i}kx} \, \mathrm{d}x. \tag{3.7}$$

The transform of (3.3) leads to

$$\frac{\mathrm{d}^2 \hat{\Phi}^a}{\mathrm{d}y^2} - l^2 \hat{\Phi}^a = 0 \quad \text{in } -H/2 < y < H/2, \tag{3.8}$$

with $l = (k^2 - \omega^2/a_0^2)^{1/2}$. Setting $B/2$ and $H/2$ to be b and h, respectively, the boundary conditions are transformed into

$$\frac{\partial \hat{\Phi}^a}{\partial y} = \frac{1}{\sqrt{2\pi}} \int_{-b}^{+b} W^a \mathrm{e}^{\mathrm{i}kx} \, \mathrm{d}x = \frac{2W^a}{\sqrt{2\pi}} \frac{\sin(kb)}{k} \quad \text{at} \quad y = \pm h, \tag{3.9}$$

where W^a is assumed uniform over the width of the throat. Thus $\hat{\Phi}$ is easily obtained as

$$\hat{\Phi}^a = \frac{2W^a}{\sqrt{2\pi}} \frac{\sin(kb)}{kl} \frac{\sinh(ly)}{\cosh(lh)}. \tag{3.10}$$

Applying the inverse transform to this, Φ is expressed as

$$\Phi^a = \frac{W^a}{\pi} \int_{-\infty}^{\infty} \frac{\sin(kb)}{kl} \frac{\sinh(ly)}{\cosh(lh)} \mathrm{e}^{-\mathrm{i}kx} \, \mathrm{d}k. \tag{3.11}$$

Because the integrand is odd with respect to k, the imaginary part vanishes on integration. While Φ^a is anti-symmetric with respect to y, i.e. $\Phi^a(x, -y) = -\Phi^a(x, y)$, it is symmetric with respect to x, i.e. $\Phi^a(-x, y) = \Phi^a(x, y)$.

Noting that $P = -\mathrm{i}\omega\rho_0\Phi(x, y)$ and using this in (3.4) with $W^+ = -W^- = W^a$, it follows that

$$BW^a = -\mathrm{i}\omega\rho_0 Y \frac{W^a}{\pi} \int_{-\infty}^{\infty} \frac{\sin(kb)}{kl} \tanh(lh) \, \mathrm{d}k. \tag{3.12}$$

Since $W^a \neq 0$, the following relation must be satisfied:

$$\frac{\omega_0^2 - \omega^2}{\omega^2} = \frac{1}{\pi L} \int_{-\infty}^{\infty} \frac{\sin(kb)}{kl} \tanh(lh) \, \mathrm{d}k. \tag{3.13}$$

This yields a frequency equation which determines the angular frequency ω.

The symmetric solution Φ^s can be sought in a similar way by taking $W^+ = W^- = W^s$. It is given as

$$\Phi^s = \frac{W^s}{\pi} \int_{-\infty}^{\infty} \frac{\sin(kb)}{kl} \frac{\cosh(ly)}{\sinh(lh)} \mathrm{e}^{-\mathrm{i}kx} \, \mathrm{d}k, \tag{3.14}$$

with $\Phi^s(x, -y) = \Phi^s(x, y)$ and $\Phi^s(-x, y) = \Phi^s(x, y)$. Imposing the relation (3.4), the frequency equation is then obtained as

$$\frac{\omega_0^2 - \omega^2}{\omega^2} = \frac{1}{\pi L} \int_{-\infty}^{\infty} \frac{\sin(kb)}{kl} \coth(lh) \, \mathrm{d}k. \tag{3.15}$$

Note that $\tanh(lh)$ in (3.13) is inverted for the symmetric mode.

3.3. *Frequency equations*

We now seek solutions to the frequency equation (3.13) for the anti-symmetric mode. First the dimensionless quantities are introduced as follows:

$$\frac{\omega H}{a_0} \equiv \sigma, \quad \frac{\omega_0 H}{a_0} \equiv \sigma_0, \quad k \equiv \frac{\omega}{a_0}\eta, \quad \frac{B}{H} \equiv \chi. \tag{3.16}$$

In terms of these, (3.13) is rewritten as

$$\frac{L}{H}\left(\frac{\sigma_0^2 - \sigma^2}{\sigma}\right) = \frac{1}{\pi}\int_{-\infty}^{\infty} \frac{\sin\left(\frac{1}{2}\chi\sigma\eta\right)}{\eta(\eta^2-1)^{1/2}} \tanh\left[\tfrac{1}{2}\sigma(\eta^2-1)^{1/2}\right] \mathrm{d}\eta. \tag{3.17}$$

It is easily seen that the integral takes a real value and does not diverge in the limits as $\eta \to 0$ and $\eta \to \pm\infty$ because the integrand behaves as $\eta^{-2}\sin(\chi\sigma\eta/2)$ in the latter limit. Whereas $(\eta^2-1)^{1/2}$ has branch points at $\eta = \pm 1$, the integrand behaves regularly as a whole at $\eta = \pm 1$ because of the factor $\tanh[(\sigma/2)(\eta^2-1)^{1/2}]$. Rather, it should be noted that the integrand has simple poles at $(\sigma/2)(\eta^2-1)^{1/2} = \pm\mathrm{i}(2n-1)\pi/2$ ($n = 1, 2, 3, \ldots$) where $\tanh[(\sigma/2)(\eta^2-1)^{1/2}]$ diverges, i.e. $\cosh[(\sigma/2)(\eta^2-1)^{1/2}]$ vanishes. These poles are given by

$$\eta = \pm\frac{\mathrm{i}}{\sigma}[(2n-1)^2\pi^2 - \sigma^2]^{1/2} \equiv \pm\eta_n. \tag{3.18}$$

These are located on the real axis of the complex η-plane or on the imaginary axis, depending on the value of σ. When $\sigma > \pi$, some poles are on the real axis and then the integral diverges in the ordinary sense. Then (3.17) obviously has no solutions. The definition of the integral in this case will be discussed later by taking detours around the poles. But it will turn out that σ should be smaller than π, i.e. the lowest cutoff frequency.

For $\sigma < \pi$, all poles are located on the imaginary axis and the integral on the right-hand side of (3.17), denoted by $I^a(\sigma, \chi)$, is evaluated as follows. Setting $\sin(\chi\sigma\eta/2) = [\exp(\mathrm{i}\chi\sigma\eta/2) - \exp(-\mathrm{i}\chi\sigma\eta/2)]/2\mathrm{i}$, the integral on the right-hand side of (3.17) is transformed into

$$I^a = \frac{1}{\pi\mathrm{i}}\mathrm{P}\int_{-\infty}^{\infty} \frac{\mathrm{e}^{\mathrm{i}\chi\sigma\eta/2}}{\eta(\eta^2-1)^{1/2}} \tanh\left[\tfrac{1}{2}\sigma(\eta^2-1)^{1/2}\right] \mathrm{d}\eta. \tag{3.19}$$

This integral is defined by taking Cauchy's principal value at $\eta = 0$, designated by P, since there is no singularity in (3.17) originally. To invoke Cauchy's integral theorem to evaluate I^a, auxiliary semicircles of infinite radius and of infinitesimally small radius both centred at $\eta = 0$ are introduced in the upper half-η-plane and (3.19) is regarded as part of the integral along a closed contour. This integral is calculated by taking account of the residues at the poles $\eta = \eta_n$ ($n \geqslant 1$) and the integral around the pole $\eta = 0$. In the vicinity of the former poles, the integrand behaves as

$$\frac{2\mathrm{e}^{\mathrm{i}\chi\sigma\eta/2}}{\sigma\eta_n^2(\eta - \eta_n)} \quad \text{as} \quad \eta \to \eta_n, \tag{3.20}$$

while as $\eta \to 0$ it behaves as $\tan(\sigma/2)/\eta$. Thus I^a is evaluated as

$$I^a = \tan\left(\frac{\sigma}{2}\right) - \sum_{n=1}^{\infty} \frac{4\sigma}{(2n-1)^2\pi^2 - \sigma^2} \exp\left[-\tfrac{1}{2}\chi\sqrt{(2n-1)^2\pi^2 - \sigma^2}\right]; \tag{3.21}$$

note the sign and the magnitude of the integral around the pole at $\eta = 0$, and that the contribution from the semicircle of infinite radius vanishes.

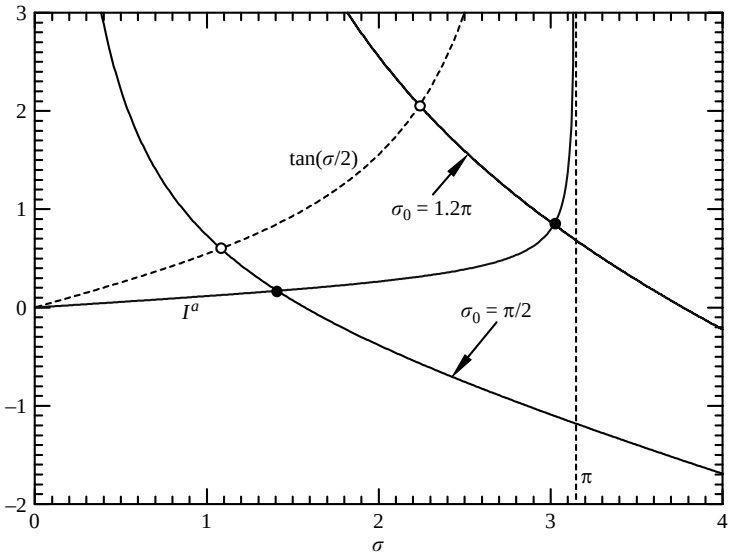

FIGURE 4. Graphical solution to the frequency equation (3.17) for the case with $L/H = 0.5$ and $\chi = 0.1$ where each side of the equation is drawn against σ as solid lines; the left-hand side is drawn for two cases labelled $\sigma_0 = \pi/2$ and $\sigma_0 = 1.2\pi$, while the right-hand side is labelled I^a; the frequency at each intersection indicated by solid circle gives $\sigma = 1.4098$ for $\sigma_0 = \pi/2$ and 3.0183 for $\sigma_0 = 1.2\pi$; the intersections with the broken line $\tan(\sigma/2)$ indicated by the open circle give the respective lower bounds of the frequency in the limit as $\chi \to \infty$.

As is seen from the integral of (3.17), I^a should vanish as $\chi \to 0$. In fact, the following identity holds (see, for example, Morse & Feshbach 1953, Chap. 4, p. 384):

$$\tan\left(\frac{\sigma}{2}\right) = \sum_{n=1}^{\infty} \frac{4\sigma}{(2n-1)^2\pi^2 - \sigma^2}. \tag{3.22}$$

Using this, I^a is rewritten as

$$I^a = \sum_{n=1}^{\infty} \frac{4\sigma}{(2n-1)^2\pi^2 - \sigma^2} \left\{1 - \exp\left[-\tfrac{1}{2}\chi\sqrt{(2n-1)^2\pi^2 - \sigma^2}\right]\right\}. \tag{3.23}$$

As χ increases from zero, I^a grows monotonically to take the value $\tan(\sigma/2)$ in the limit as $\chi \to \infty$. It is found from (3.23) that I^a, which is positive for $0 < \sigma < \pi$, diverges as $\sigma \to \pi$, while it vanishes as $\sigma \to 0$.

It is instructive to solve (3.17) graphically. Figure 4 shows graphs of the left- and right-hand sides of (3.17) with respect to σ as solid lines for a case with $L/H = 0.5$ and $\chi = 0.1$ where the left-hand side is drawn for two values of $\sigma_0 = \pi/2$ and 1.2π. For each value of σ_0, there occurs only one intersection, marked by the solid circle, giving one solution for σ. The intersection may be classified according to whether σ_0 is lower than π or not. When $\sigma_0 < \pi$, the frequency at the intersection is just below σ_0 ($= \pi/2$) and found numerically to be 1.4098. When $\sigma_0 > \pi$, on the other hand, the frequency is just below π and found numerically to be 3.0183. In this case, the frequency is far below σ_0 ($= 1.2\pi$). In either case, the frequency at the intersection is lower than the cutoff frequency and also the natural frequency of the resonator.

The intersection varies with the value of χ or L/H. As χ tends to vanish, the frequency approaches σ_0, if σ_0 is lower than π. Designating I^a at $\sigma = \sigma_0$ as α^a, the

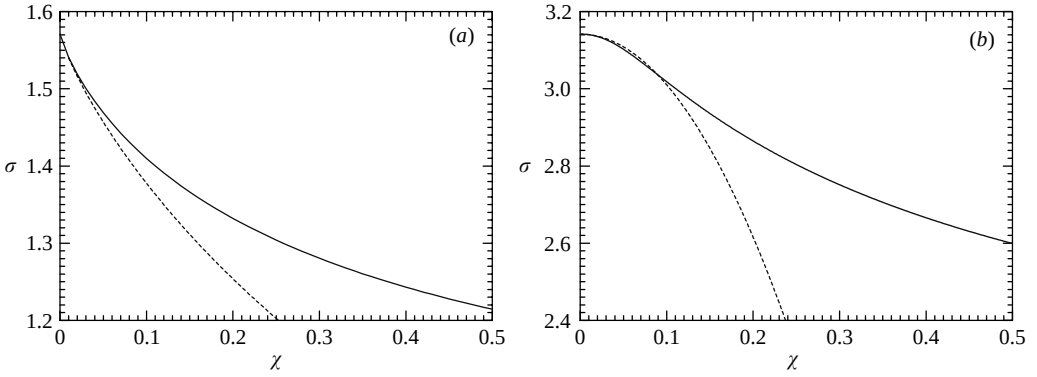

FIGURE 5. Parametric dependence of the solution to (3.17) on χ with $L/H = 0.5$ and σ_0 fixed where the solid lines in (*a*) and (*b*) represent the numerical solutions in the cases with $\sigma_0 = \pi/2$ and $\sigma_0 = 1.2\pi$, respectively, while the broken lines represent the respective approximate solutions (3.24) and (3.25).

solution of (3.17) for $\chi \ll 1$ is obtained approximately as

$$\sigma = \sigma_0 - \frac{\alpha^a H}{2L} + \cdots. \tag{3.24}$$

If σ_0 is higher than π, then σ is obtained as

$$\sigma = \pi - \frac{2\pi^3 \chi^2 H^2}{\left(\sigma_0^2 - \pi^2\right)^2 L^2} + \cdots. \tag{3.25}$$

As the value of χ is increased with L/H and σ_0 fixed, on the other hand, the frequency becomes lower. The broken line in figure 4 indicates the limiting value of I^a as $\chi \to \infty$, i.e. $\tan(\sigma/2)$. The intersection with the broken line, marked by the open circle, gives the lower bound of the frequency. Figures 5(*a*) and 5(*b*) show the solutions to (3.17) with $L/H = 0.5$ fixed against the value of χ ($0 < \chi \leqslant 0.5$) for $\sigma_0 = \pi/2$ and $\sigma_0 = 1.2\pi$, respectively, where the solid lines represent the numerical solutions, and the broken lines the respective approximate solutions (3.24) and (3.25). It is seen in figure 5(*a*) that the numerical solution for σ at $\chi = 0.5$ is close to the lower bound, about $\sigma \approx 1.1$ (see figure 4), while (3.24) and (3.25) provide good approximations for a small value of χ. Note that since the values of σ_0 and L/H are fixed, a change in χ corresponds to that in S as well as B. If the value of L/H is decreased with σ_0 and χ fixed, (3.24) and (3.25) suggest that the frequency is lowered.

3.4. *Pressure distribution*

As the frequency determined by (3.17) is lower than all cutoff frequencies, it is expected from figure 1 that the sound field will be represented by the lowest propagating mode with $m = 0$ and the evanescent modes. It is obvious, however, that the propagating mode does not come into play, because the pressure field should be anti-symmetric with respect to y.

To see this quantitatively, we seek Φ^a by evaluating the integral (3.11). Normalizing x, y and Φ^a by setting these to be HX, HY and $(a_0 W^a/\omega)J$, respectively, J is expressed as

$$J = \frac{1}{\pi} \int_{-\infty}^{\infty} \frac{\sin\left(\frac{1}{2}\chi\sigma\eta\right)}{\eta(\eta^2-1)^{1/2}} \frac{\sinh\left[\sigma Y(\eta^2-1)^{1/2}\right]}{\cosh\left[\frac{1}{2}\sigma(\eta^2-1)^{1/2}\right]} \exp(-\mathrm{i}\sigma X\eta)\,\mathrm{d}\eta. \tag{3.26}$$

This integral can be evaluated in the same way as I^a. Decomposing $\sin(\chi\sigma\eta/2)$ into the sum of two exponential functions, and noting that the integrand is regular at $\eta = 0$, (3.26) is expressed as follows:

$$J = \frac{1}{2\pi i}\mathrm{P}\int_{-\infty}^{\infty} \frac{1}{\eta(\eta^2-1)^{1/2}} \frac{\sinh\left[\sigma Y(\eta^2-1)^{1/2}\right]}{\cosh\left[\frac{1}{2}\sigma(\eta^2-1)^{1/2}\right]} \exp[-i\sigma(X-\chi/2)\eta]\,d\eta$$
$$-\frac{1}{2\pi i}\mathrm{P}\int_{-\infty}^{\infty} \frac{1}{\eta(\eta^2-1)^{1/2}} \frac{\sinh\left[\sigma Y(\eta^2-1)^{1/2}\right]}{\cosh\left[\frac{1}{2}\sigma(\eta^2-1)^{1/2}\right]} \exp[-i\sigma(X+\chi/2)\eta]\,d\eta. \quad (3.27)$$

Both integrals are extended as parts of the ones along closed contours. According to whether the factors $X - \chi/2$ and $X + \chi/2$ are positive or negative, auxiliary semicircles of infinite radius and infinitesimally small radius centred at $\eta = 0$ are taken, respectively, in the lower or upper half-η-plane. Therefore four cases arise but the calculations are straightforwardly done. The results are given as follows: for the domain $|X| > \chi/2$

$$J = \sum_{n=1}^{\infty} \frac{2(-1)^n\sigma}{\lambda_n^2} \sin[(2n-1)\pi Y]\{\exp[-(|X|+\chi/2)\lambda_n] - \exp[-(|X|-\chi/2)\lambda_n]\}, \quad (3.28)$$

while for the domain $|X| < \chi/2$

$$J = \frac{\sin(\sigma Y)}{\cos(\sigma/2)} + \sum_{n=1}^{\infty} \frac{2(-1)^n\sigma}{\lambda_n^2} \sin[(2n-1)\pi Y]\{\exp[(|X|-\chi/2)\lambda_n] + \exp[-(|X|+\chi/2)\lambda_n]\}, \quad (3.29)$$

with $\lambda_n = [(2n-1)^2\pi^2 - \sigma^2]^{1/2}$.

It is found from (3.28) and (3.29) that no propagating mode is involved and that J is expressed in terms of the anti-symmetric evanescent modes only. In fact, noting that $(-1)^n \sin[(2n-1)\pi Y] = \cos[(2n-1)\pi(Y+1/2)]$, J is expressed in terms of the odd evanescent modes only. Thus Φ^a vanishes as $|X| \to \infty$ so that it is localized around the resonator. The absence of the lowest propagating mode means the absence of radiation damping, which makes the localization possible. Therefore it is conjectured that no localization occurs in the symmetric mode.

Figure 6 shows the profile of J over $|X| \leqslant 2$ and $|Y| \leqslant 0.5$ for the case with $\chi = 0.1$ and $\sigma \approx 1.4098$ ($L/H = 0.5$ and $\sigma_0 = \pi/2$). Since the pressure is proportional to Φ^a, the figure represents the pressure distribution, apart from the scale. Thus the pressure field is anti-symmetric spanwise with respect to the centreline of the waveguide but symmetric with respect to the axial direction. At the junctions $|X| = \chi/2$, it is found that (3.28) agrees with (3.29) by noting the Fourier expansion

$$\frac{\sin(\sigma Y)}{\cos(\sigma/2)} = -\sum_{n=1}^{\infty} \frac{4(-1)^n\sigma}{(2n-1)^2\pi^2 - \sigma^2} \sin[(2n-1)\pi Y]. \quad (3.30)$$

Further $\partial J/\partial X$ and $\partial J/\partial Y$ are also found to be continuous across $|X| = \chi/2$ for $|Y| < H/2$. Finally it is noted that if the frequency of localized oscillations is close to the cutoff frequency π for $\sigma_0 > \pi$, then the localization becomes weaker because λ_1 becomes smaller.

3.5. *Evaluation of the integral I^a for $\pi < \sigma < 3\pi$*

In the evaluation of I^a, σ is required to be lower than the lowest cutoff frequency π. If some poles are located just on the real axis of η, then the integral diverges in the ordinary sense. To define the integral in this case, the lossless case is regarded as

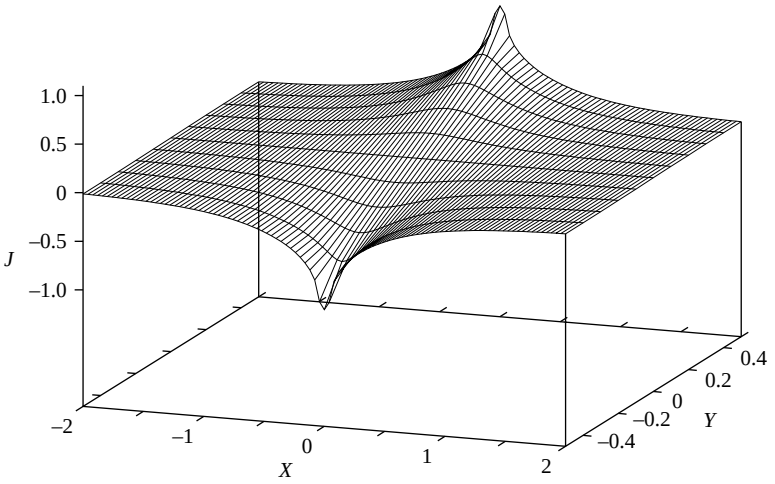

FIGURE 6. Localized profile of J for $\sigma = 1.4098$ in the (X, Y)-space, corresponding to the pressure distribution, apart from the scale.

a limit of the lossy case and small damping is introduced to shift the poles off the real axis. This clarifies a geometrical relation between the poles and the integral path. Then by taking lossless limit, the integral may be evaluated.

The damping is taken into account artificially by considering the following equation in place of (2.1) (Noble 1988, p. 28):

$$\frac{\partial^2 \phi}{\partial t^2} + \varepsilon \frac{\partial \phi}{\partial t} = a_0^2 \left(\frac{\partial^2 \phi}{\partial x^2} + \frac{\partial^2 \phi}{\partial y^2} \right), \tag{3.31}$$

where the second term on the left-hand side accounts for the artificial damping and $0 < \varepsilon/\omega \ll 1$ for an appropriate value of ω. This is a mathematically simple procedure to take account of damping. Physically, however, dissipative effects on sound in a waveguide are due to a boundary layer and diffusivity of sound, which are taken into account in a different form (see (60) with $\kappa = 0$ in Sugimoto & Horioka 1995). With the damping included, the factor $(\eta^2 - 1)^{1/2}$ in (3.19) is now replaced by $(\eta^2 - 1 + \mathrm{i}\varepsilon H/a_0\sigma)^{1/2}$.

Suppose a case with $\pi < \sigma < 3\pi$. The simple poles at $\eta = \pm\eta_1$ $(= \pm\sqrt{1 - \pi^2/\sigma^2})$ are shifted to

$$\eta = \pm \left(1 - \frac{\pi^2}{\sigma^2}\right)^{1/2} \left[1 - \frac{\mathrm{i}\varepsilon H}{2a_0\sigma(1 - \pi^2/\sigma^2)} + \cdots\right], \tag{3.32}$$

as shown by the crosses in figure 7. When the limit as $\varepsilon \to 0$ is taken, the poles tend to fall on the real axis as indicated by arrows in figure 7. Then the integral path along the real axis is indented around them by semicircles of infinitesimally small radius as in figure 7. When I^a is evaluated with the aid of the auxiliary semicircles in the upper half-η-plane, the contribution from the pole at $\eta = -\eta_1$ must be taken into account. Then (3.21) is modified to include $(4/\sigma\eta_1^2)\exp(-\mathrm{i}\chi\sigma\eta_1/2)$ and the summation begins with $n = 2$. Unless $\sin(\chi\sigma\eta_1/2)$ vanishes, I^a becomes complex and then the frequency equation (3.17) has no real roots. If it vanishes, then $\chi\sigma\eta_1/2$ $(= \chi\sqrt{\sigma^2 - \pi^2}/2)$ must be equal to a multiple of π. Since the value of χ is usually much smaller than unity, there exists no such a value of σ. Thus σ is required to be lower than π.

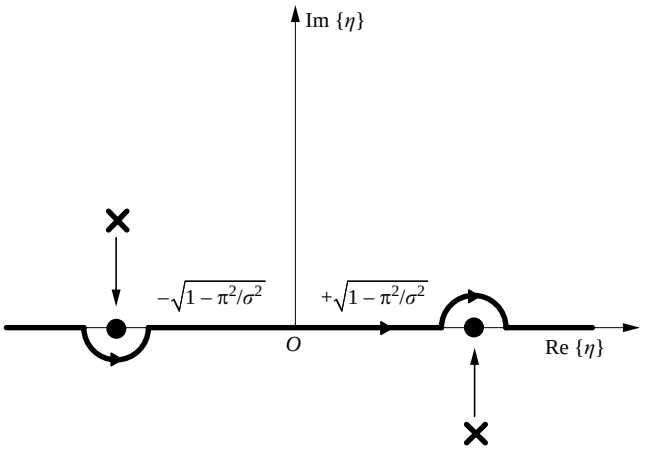

FIGURE 7. Determination of the integral path, where the cross indicates the simple poles (3.32) slightly shifted from $\eta = \pm\sqrt{1-\pi^2/\sigma^2} = \pm\eta_1$ with $\pi < \sigma$ by inclusion of the small artificial damping ε, and the indented paths around the poles are drawn in the thick lines in the limit as $\varepsilon \to 0$.

4. Cases of non-existent localized mode

This section examines possibilities of localized oscillations in the symmetric mode and in the case of a waveguide with resonators offset on the wall.

4.1. *The symmetric mode*

The frequency equation (3.15) for the symmetric mode is considered. It is given in dimensionless form as

$$\frac{L}{H}\left(\frac{\sigma_0^2-\sigma^2}{\sigma}\right) = \frac{1}{\pi}\int_{-\infty}^{\infty} \frac{\sin\left(\frac{1}{2}\chi\sigma\eta\right)}{\eta(\eta^2-1)^{1/2}} \coth\left[\tfrac{1}{2}\sigma(\eta^2-1)^{1/2}\right] \mathrm{d}\eta. \tag{4.1}$$

This is reduced to equation (3.19) with tanh[...] replaced by coth[...]. Simple poles appear at $\eta = \pm 1$ on the real axis. Inclusion of the small dissipation shifts the poles slightly to

$$\eta = \pm\left(1 - \frac{\mathrm{i}\varepsilon H}{2a_0\sigma} + \cdots\right). \tag{4.2}$$

Thus the small detours around $\eta = \pm 1$ are taken similarly to those in figure 7. Denoting the integral on the right-hand side of (4.1) by $I^s(\sigma, \chi)$, it is calculated to be

$$I^s = -\cot\left(\frac{\sigma}{2}\right) - \sum_{n=1}^{\infty} \frac{4\sigma}{(2\pi n)^2-\sigma^2} \exp\left[-\tfrac{1}{2}\chi\sqrt{(2\pi n)^2-\sigma^2}\right] + \frac{2}{\sigma}\exp(-\mathrm{i}\chi\sigma/2). \tag{4.3}$$

The last term results from the contribution of the pole at $\eta = -1$. Because the right-hand side of (4.1) becomes complex, no real solutions exist for σ. This result is rather obvious. If a real frequency were to exist, then the pressure field would be represented by the symmetric propagating and evanescent modes. Then the plane-wave mode would be excited. Since this mode carries energy out by radiation, localization would be broken by damping.

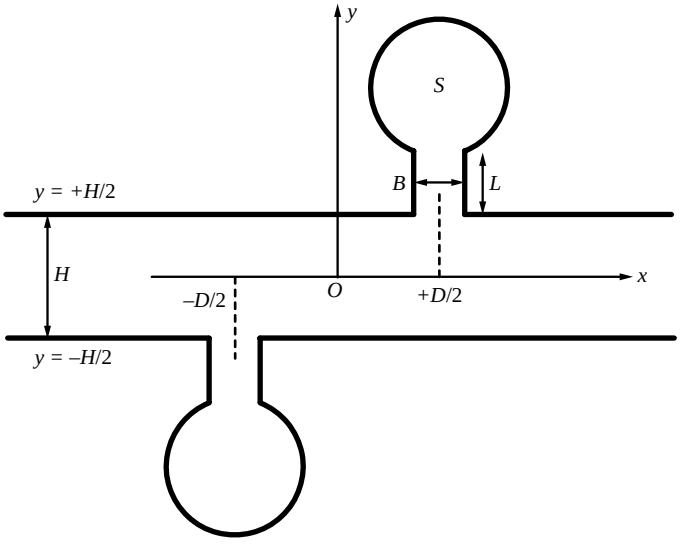

FIGURE 8. A waveguide with a pair of identical Helmholtz resonators connected to the upper and lower walls and offset axial distance D apart in the two-dimensional configuration.

Incidentally we can check the damping rate of the oscillations for a small value of χ. Noting the formula derived from (3.22) with σ shifted to $\sigma + \pi$

$$-\cot\left(\frac{\sigma}{2}\right) = \sum_{n=1}^{\infty} \frac{4\sigma}{(2\pi n)^2 - \sigma^2} - \frac{2}{\sigma}, \tag{4.4}$$

I^s may be approximated as

$$I^s = \sum_{n=1}^{\infty} \frac{4\sigma}{(2\pi n)^2 - \sigma^2} \left\{1 - \exp\left[-\tfrac{1}{2}\chi\sqrt{(2\pi n)^2 - \sigma^2}\right]\right\} - \mathrm{i}\chi + O(\chi^2), \tag{4.5}$$

where I^s tends to diverge as $\sigma \to 2\pi$.

Substituting (4.5) into (4.1) to solve for σ, and designating the real part of (4.5) at $\sigma = \sigma_0$ (assumed smaller than 2π) by α^s ($= O(\chi) \ll 1$), σ is obtained as $\sigma_0 - H\alpha^s/2L + \mathrm{i}\chi H/2L$. Thus the frequency is given in the dimensional form as

$$\omega = \omega_0 - \frac{a_0}{2L}\alpha^s + \mathrm{i}\frac{a_0 B}{2LH}. \tag{4.6}$$

The problem considered in § 2.3 is equivalent to the present one if the half-domain in $y \geqslant 0$ is concerned. Noting that half the waveguide width $H/2$ in the present context corresponds to the full one H in the previous problem, the imaginary part of (4.6) agrees with that of (2.14). But the real part is slightly lower than ω_0. This discrepancy results from the fact that the elementary theory in § 2.3 neglects the evanescent modes.

4.2. *A waveguide with the resonators offset*

We next consider a waveguide with the resonators offset, as shown in figure 8, with distance D between two centrelines of the throat (indicated by the broken lines). The boundary conditions corresponding to (3.5) are replaced by

$$\frac{\partial \Phi}{\partial y} = \begin{cases} +W^+ & \text{for} \quad |x - D/2| < B/2 \quad \text{at} \quad y = +H/2, \\ -W^- & \text{for} \quad |x + D/2| < B/2 \quad \text{at} \quad y = -H/2, \end{cases} \tag{4.7}$$

and otherwise $\partial\Phi/\partial y = 0$ at $y = \pm H/2$. Focusing on the anti-symmetric mode with $W^+ = -W^- = W^a$, (3.9) is modified as

$$\frac{\partial\hat{\Phi}^a}{\partial y} = \frac{2W^a}{\sqrt{2\pi}}\frac{\sin(kb)}{k}\mathrm{e}^{\pm \mathrm{i}kd} \quad \text{at} \quad y = \pm h, \tag{4.8}$$

with $d = D/2$. Following the same procedure as used before, Φ^a is obtained as follows:

$$\Phi^a = \frac{W^a}{\pi}\int_{-\infty}^{\infty}\frac{\sin(kb)}{kl}\left[\cos(kd)\frac{\sinh(ly)}{\cosh(lh)} + \mathrm{i}\sin(kd)\frac{\cosh(ly)}{\sinh(lh)}\right]\mathrm{e}^{-\mathrm{i}kx}\,\mathrm{d}k, \tag{4.9}$$

with $\Phi^a(-x, -y) = -\Phi^a(x, y)$. Since the response of the resonators is given by $\pm BW^a = YP(x = \pm d, y = \pm h)$, it follows that

$$\frac{\omega_0^2 - \omega^2}{\omega^2} = \frac{1}{\pi L}\int_{-\infty}^{\infty}\frac{\sin(kb)}{kl}[\cos^2(kd)\tanh(lh) + \sin^2(kd)\coth(lh)]\,\mathrm{d}k. \tag{4.10}$$

Using the dimensionless quantities (3.16) and setting D/H to be δ ($> \chi$), (4.10) is written as

$$\frac{L}{H}\left(\frac{\sigma_0^2 - \sigma^2}{\sigma}\right) = \frac{1}{\pi}\int_{-\infty}^{\infty}\frac{\sin\left(\frac{1}{2}\chi\sigma\eta\right)}{\eta(\eta^2-1)^{1/2}}\left\{\cos^2\left(\tfrac{1}{2}\delta\sigma\eta\right)\tanh\left[\tfrac{1}{2}\sigma(\eta^2-1)^{1/2}\right] + \sin^2\left(\tfrac{1}{2}\delta\sigma\eta\right)\coth\left[\tfrac{1}{2}\sigma(\eta^2-1)^{1/2}\right]\right\}\mathrm{d}\eta. \tag{4.11}$$

Rewriting the products of trigonometric functions into their sum, and using the definitions of $I^a(\sigma, \chi)$ and $I^s(\sigma, \chi)$, the right-hand side of (4.11) is expressed as

$$[2I^a(\sigma,\chi) + 2I^s(\sigma,\chi) + I^a(\sigma, 2\delta+\chi) - I^s(\sigma, 2\delta+\chi) - I^a(\sigma, 2\delta-\chi) + I^s(\sigma, 2\delta-\chi)]/4. \tag{4.12}$$

For $\sigma < \pi$, the imaginary part results from I^s, yielding $[\cos(\delta\sigma) - 1]\sin(\chi\sigma/2)/\sigma$. For $\pi < \sigma < 2\pi$, the new term $-2[\cos(\delta\sigma\eta_1) + 1]\sin(\chi\sigma/2)/\sigma\eta_1^2$ is added to the imaginary part for $\sigma < \pi$, and so on. The imaginary part does not vanish generally for a real solution of σ determined from the balance of the real part of (4.11). In other words, there exists no real solution for general geometry. But if the value of δ were to make the imaginary part vanish, then a real solution exists. For $\sigma < \pi$, this occurs for a particular spacing $\delta = 2\pi/\sigma \approx 4.35$ at $\sigma \approx 1.45$ in the case with $\sigma_0 = \pi/2$, whereas for $\pi < \sigma < 2\pi$, the imaginary part is found numerically to be always negative for $\chi = 0.1$ and $\delta < 10$. The latter suggests the existence of no frequency embedded in the continuous spectrum. But the search for such a frequency for all possible values of the parameters L/H and χ, and further beyond 2π needs a large amount of numerical computations and is beyond the scope of the present paper.

5. Generalization to cases of multiple pairs of resonators

It is anticipated from the results in the preceding sections that the localized mode would appear if multiple pairs of resonators are connected. As a simple example, we consider the waveguide as shown in figure 9 where two pairs of identical resonators opposite to each other in the walls are connected with axial distance D apart, where the right-hand pair may be different from the left in size. The quantities pertaining to each pair are designated by the subscript 1 and 2, respectively. Taking the origin of the x-axis at the midpoint between the respective centrelines of the throat, and

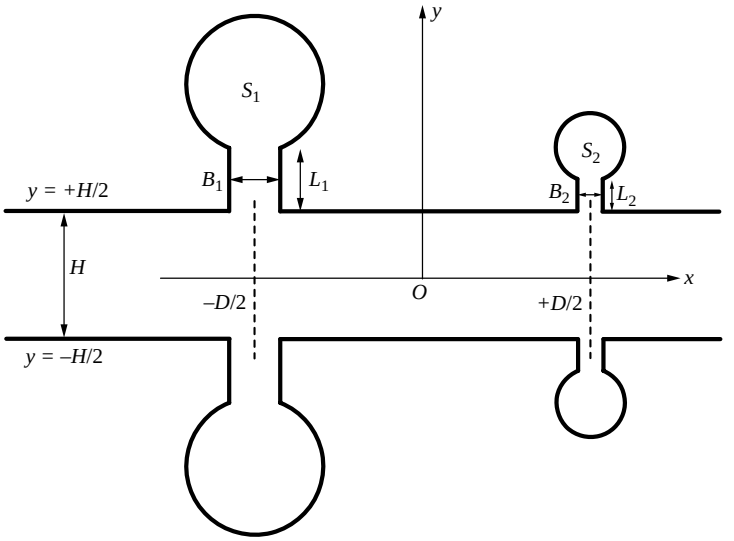

FIGURE 9. A waveguide with two pairs of identical Helmholtz resonators connected opposite each other in the upper and lower walls and axial distance D apart in the two-dimensional configuration where the left- and right-hand pairs may be different from each other in size.

assuming the anti-symmetric mode, the boundary conditions are given as follows:

$$\frac{\partial \Phi^a}{\partial y} = \begin{cases} W_1^a & \text{for } |x + D/2| < B_1/2 \text{ at } y = \pm H/2, \\ W_2^a & \text{for } |x - D/2| < B_2/2 \text{ at } y = \pm H/2, \end{cases} \tag{5.1}$$

and otherwise $\partial \Phi/\partial y = 0$ at $y = \pm H/2$ where W_1^a and W_2^a are constants to be determined. Following the same procedure as was previously used, Φ^a is obtained as

$$\Phi^a = \frac{W_1^a}{\pi} \int_{-\infty}^{\infty} \frac{\sin(kb_1)}{kl} \frac{\sinh(ly)}{\cosh(lh)} e^{-ik(x+d)}\, dk + \frac{W_2^a}{\pi} \int_{-\infty}^{\infty} \frac{\sin(kb_2)}{kl} \frac{\sinh(ly)}{\cosh(lh)} e^{-ik(x-d)}\, dk, \tag{5.2}$$

with $b_1 = B_1/2$, $b_2 = B_2/2$ and $d = D/2$. Here Φ^a is anti-symmetric with respect to y but asymmetric in general with respect to x. Imposing the conditions for connection of the resonators, $\pm B_1 W_1^a = Y_1 P(x = -d, y = \pm h)$ and $\pm B_2 W_2^a = Y_2 P(x = +d, y = \pm h)$, with the respective acoustic admittances defined similarly to (2.10) as

$$Y_1 = \frac{B_1}{\rho_0 L_1} \left(\frac{i\omega}{\omega_1^2 - \omega^2} \right) \quad \text{and} \quad Y_2 = \frac{B_2}{\rho_0 L_2} \left(\frac{i\omega}{\omega_2^2 - \omega^2} \right), \tag{5.3}$$

ω_1 and ω_2 being the natural angular frequencies of the respective resonators, it follows that two relations must hold simultaneously:

$$\frac{\omega_1^2 - \omega^2}{\omega^2} W_1^a = \frac{1}{\pi L_1} \int_{-\infty}^{\infty} \left[W_1^a \frac{\sin(kb_1)}{kl} + W_2^a \frac{\sin(kb_2)}{kl} e^{2ikd} \right] \tanh(lh)\, dk, \tag{5.4}$$

and

$$\frac{\omega_2^2 - \omega^2}{\omega^2} W_2^a = \frac{1}{\pi L_2} \int_{-\infty}^{\infty} \left[W_1^a \frac{\sin(kb_1)}{kl} e^{-2ikd} + W_2^a \frac{\sin(kb_2)}{kl} \right] \tanh(lh)\, dk. \tag{5.5}$$

In order that W_1^a and W_2^a are non-trivial, a relation among their coefficients must be satisfied, which gives the frequency equation.

Before deriving it, we introduce dimensionless quantities in addition to (3.16) as follows:

$$\frac{\omega_1 H}{a_0} \equiv \sigma_1, \quad \frac{\omega_2 H}{a_0} \equiv \sigma_2, \quad \frac{B_1}{H} \equiv \chi_1, \quad \frac{B_2}{H} \equiv \chi_2, \quad \frac{D}{H} \equiv \delta. \tag{5.6}$$

Furthermore defining I_n and K_n $(n = 1, 2)$ to be

$$I_n \equiv \frac{1}{\pi} \int_{-\infty}^{\infty} \frac{\sin\left(\frac{1}{2}\chi_n \sigma \eta\right)}{\eta(\eta^2 - 1)^{1/2}} \tanh\left[\tfrac{1}{2}\sigma(\eta^2 - 1)^{1/2}\right] \mathrm{d}\eta, \tag{5.7}$$

and

$$K_n \equiv \frac{1}{\pi} \int_{-\infty}^{\infty} \frac{\sin\left(\frac{1}{2}\chi_n \sigma \eta\right)}{\eta(\eta^2 - 1)^{1/2}} \cos(\delta\sigma\eta) \tanh\left[\tfrac{1}{2}\sigma(\eta^2 - 1)^{1/2}\right] \mathrm{d}\eta, \tag{5.8}$$

respectively, relations (5.4) and (5.5) are rewritten as

$$F_1 W_1^a - K_2 W_2^a = 0 \quad \text{and} \quad -K_1 W_1^a + F_2 W_2^a = 0, \tag{5.9}$$

with

$$F_1 \equiv \frac{L_1}{H}\left(\frac{\sigma_1^2 - \sigma^2}{\sigma}\right) - I_1 \quad \text{and} \quad F_2 \equiv \frac{L_2}{H}\left(\frac{\sigma_2^2 - \sigma^2}{\sigma}\right) - I_2, \tag{5.10}$$

and the frequency equation is given in the following dimensionless form:

$$F_1 F_2 - K_1 K_2 = 0. \tag{5.11}$$

Here it should be remarked that as δ becomes larger than unity, the integrals K_1 and K_2 tend to vanish because destructive cancellation occurs due to the factor $\cos(\delta\sigma\eta)$, except for the vicinity of $\sigma = \pi$. Thus if two pairs are connected with axial distance large enough, then two factors F_1 and F_2 vanish separately to yield the respective frequencies of the localized oscillations. Conversely as the distance between two pairs becomes smaller, though $(\chi_1 + \chi_2)/2 \ll \delta$, the respective frequencies tend to be modified.

Figure 10 shows the graphs of the product of F_1 and F_2 and that of K_1 and K_2 versus σ as solid lines with F_1 and F_2 as broken lines for the following values of the parameters: $L_1/H = 0.5$, $L_2/H = 0.25$, $\sigma_1 = \pi/2$, $\sigma_2 = 1.2\pi$, $\chi_1 = 0.1$, $\chi_2 = 0.05$ and $\delta = 0.5$. There exist two intersections between the curves F_1F_2 and K_1K_2 marked by the solid circles in figure 10. The frequencies are close to the respective ones of $F_1 = 0$ and $F_2 = 0$ in the case of the single pair, which are given, respectively, by the intersections between curve F_1F_2 and the broken lines. Even for the small value of $\delta = 0.5$, the effect of the double pair remains small. Because both K_1 and K_2 take positive, small values, it is found graphically that one frequency is slightly lower than the one determined by $F_1 = 0$ whereas the other is slightly higher than the one by $F_2 = 0$. For the respective frequencies, it follows that $W_2^a/W_1^a = F_1/K_2 = K_1/F_2$. For the lower frequency, F_1 and K_2 are positive so that W_2^a/W_1^a is also positive and the localized oscillations around the left-hand pair are in phase with the ones around the right-hand pair. For the higher frequency, however, F_1 is negative so that W_2^a/W_1^a is also negative and both localized oscillations are out of phase by π.

An interesting case occurs when the two pairs are identical. Since the frequency of the localized oscillations is common, is this frequency subject to change? Setting

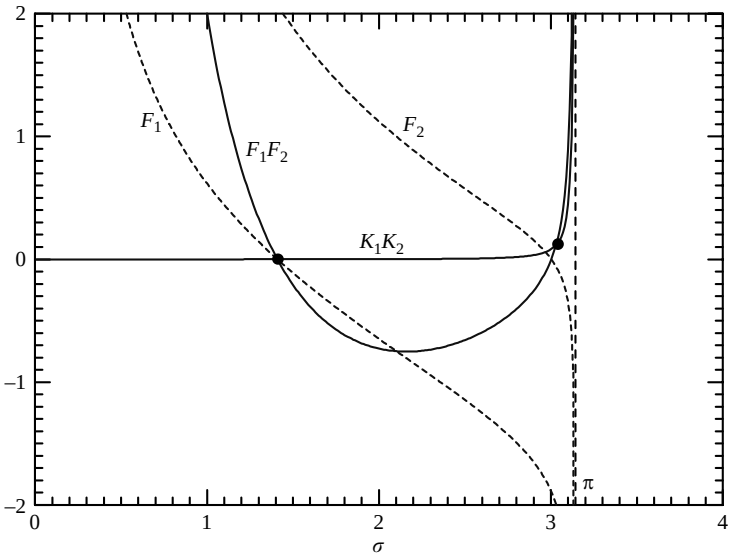

FIGURE 10. Graphs of F_1F_2 and K_1K_2 versus σ as solid lines with F_1 and F_2 as broken lines for the values of the parameters $L_1/H = 0.5$, $L_2/H = 0.25$, $\sigma_1 = \pi/2$, $\sigma_2 = 1.2\pi$ $\chi_1 = 0.1$, $\chi_2 = 0.05$ and $\delta = 0.5$ where the solid circles indicate the intersections between curves F_1F_2 and K_1K_2, which give the frequencies of the localized oscillations slightly lower and higher than the ones determined by $F_1 = 0$ and $F_2 = 0$, respectively.

$L_1 = L_2 = L$, $\sigma_1 = \sigma_2 = \sigma_0$ and $\chi_1 = \chi_2 = \chi$, the frequencies for the localized oscillations are given by the roots of

$$\frac{L}{H}\left(\frac{\sigma_0^2 - \sigma^2}{\sigma}\right) = I \pm K, \tag{5.12}$$

with $I_1 = I_2 = I$ and $K_1 = K_2 = K$. Figure 11 shows graphs of the left-hand side of (5.12) and of the right-hand sides $I \pm K$ as solid lines for the values of the parameters $L/H = 0.5$, $\sigma_0 = \pi/2$, $\chi = 0.1$ and $\delta = 0.5$. The broken line represents the graph of I. As $\sigma \to \pi$, K diverges as does I. This can be seen as follows. Using $I^a(\sigma, \chi)$ for the integral on the right-hand side of (3.17), I and K are written as $I^a(\sigma, \chi)$ and $[I^a(\sigma, 2\delta + \chi) - I^a(\sigma, 2\delta - \chi)]/2$, respectively. It is found from (3.23) that K diverges to approach I so that $I - K$ is finite at $\sigma = \pi$.

The intersection of the curve labelled $\sigma_0 = \pi/2$ and the broken line gives the frequency of the localized oscillations in the case of the single pair. This may be regarded as the case in which the distance between two pairs δ is so large that K may substantially vanish. Otherwise two intersections occur between the curve labelled $\sigma_0 = \pi/2$ and the curves $I \pm K$. Thus it is found that the frequency for the single pair is split into two frequencies around it: one slightly lower and the other frequency slightly higher. The lower and upper bounds of the respective frequencies are determined by the maximum value of K. Although K becomes large as δ becomes small, note that δ should be greater than χ. At the respective intersections with the curve $I \pm K$, it follows that $W_1^a = \pm W_2^a$, the sign $\pm$ ordered vertically. Since $|W_1^a| = |W_2^a|$, it follows by symmetry that the localized oscillations around the left- and right-hand pairs are equal in magnitude. At the lower frequency, both oscillations are in phase and symmetric with respect to x, whereas at the higher frequency, they are out of

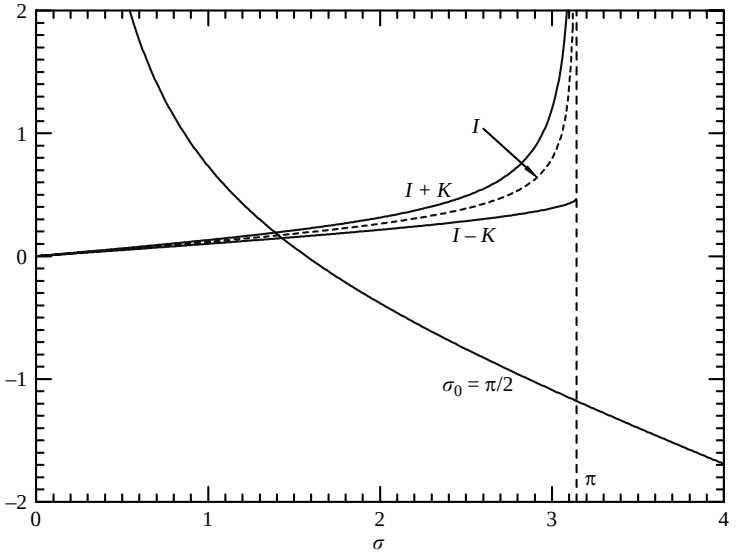

FIGURE 11. Graphs of the left-hand side of (5.12) (labelled $\sigma_0 = \pi/2$) and the right-hand side $I \pm K$ versus σ as solid lines with the graph of I as the broken line for the values of parameters $L/H = 0.5$, $\sigma_0 = \pi/2$, $\chi = 0.1$ and $\delta = 0.5$ where the intersection between the curve labelled $\sigma_0 = \pi/2$ and the broken line is split into two intersections due to K, which gives two frequencies of the localized oscillations slightly lower and higher than the one determined by the single pair.

phase by π and anti-symmetric axially. Of course, both oscillations are anti-symmetric spanwise.

Extending the above result, we finally consider the case where N ($\geqslant 3$) pairs of identical resonators are connected. Designating each pair by the subscript n ($1 \leqslant n \leqslant N$) consecutively, the axial position of the centreline of the throat of the nth pair is specified as $x_n = (n - 3/2)D = (2n - 3)d$. Thus the boundary conditions are given as follows:

$$\frac{\partial \Phi^a}{\partial y} = W_n^a \quad \text{for} \quad |x - x_n| < B/2 \quad \text{at} \quad y = \pm H/2, \tag{5.13}$$

for $n = 1, 2, \ldots, N$, and otherwise $\partial \Phi / \partial y = 0$ at $y = \pm H/2$, where W_n^a are constants to be determined. Since identical resonators are assumed, no subscript is attached to B and L and the natural angular frequency is denoted by ω_0. The solution Φ^a is obtained similarly as

$$\Phi^a = \sum_{n=1}^{N} \frac{W_n^a}{\pi} \int_{-\infty}^{\infty} \frac{\sin(kb)}{kl} \frac{\sinh(ly)}{\cosh(lh)} \mathrm{e}^{-\mathrm{i}k(x - x_n)} \, \mathrm{d}k. \tag{5.14}$$

Imposing the conditions for connection of the resonators at $x = x_m$ ($m = 1, 2, \ldots, N$), $\pm B W_m^a = YP(x = x_m, y = \pm h)$, and using the dimensionless parameters, we derive the simultaneous equations for W_n^a as follows:

$$\sum_{n=1}^{N} \mathscr{A}_{mn} W_n^a = 0 \quad (m, n = 1, 2, \ldots, N), \tag{5.15}$$

with

$$\mathscr{A}_{mn} = \frac{L}{H}\left(\frac{\sigma_0^2 - \sigma^2}{\sigma}\right)\delta_{mn} - \frac{1}{\pi}\int_{-\infty}^{\infty} \frac{\sin\left(\frac{1}{2}\chi\sigma\eta\right)}{\eta(\eta^2-1)^{1/2}} \times \cos[(m-n)\delta\sigma\eta]\tanh\left[\tfrac{1}{2}\sigma(\eta^2-1)^{1/2}\right]\,\mathrm{d}\eta, \tag{5.16}$$

where δ_{mn} denotes Kronecker's delta symbol. From the non-trivial solutions for W_n^a, the determinant of the matrix $\mathscr{A}_{mn}$ must vanish so that the frequency equation is obtained. To obtain the frequencies, the equation will have to be solved numerically. It is emphasized again that as $|(m-n)|\delta$ becomes larger, the integral tends to vanish. In view of the results for $N = 2$, we expect that N frequencies may exist and that they would be located near to the frequency for the case of the single pair. However it is uncertain whether or not the frequency equation always has N real roots, depending on the geometry. For the case of N multiple cylinders in a water-wave channel, see Evans & Porter (1997).

6. Conclusions

This paper has shown the existence of a localized mode of sound in a planar waveguide with a pair of identical Helmholtz resonators connected exactly opposite to each other in the walls by solving the two-dimensional problem fully. It is revealed from the frequency equation derived that there exists a single frequency at which the localized mode appears and this frequency is lower than the lowest cutoff frequency of the waveguide and the natural frequency of the resonator. It is also revealed that the pressure field is anti-symmetric spanwise with respect to the centreline of the waveguide, and symmetric axially with respect to the resonators. The field is expressed in terms of the infinite sum of the anti-symmetric evanescent modes and no plane-wave mode is involved. The absence of the latter mode makes it possible to localize sound without being accompanied by radiation damping. This explains why no symmetric localized mode over the width exists. In fact, a complex solution to the frequency equation appears in this case. It is also found that no localized mode exists generally in the waveguide with the resonators offset, but it can exist for a particular spacing between them. Further, the generalization to cases with multiple pairs of resonators connected opposite to each other has been considered. It is interesting that even if two pairs are identical, the frequency for the single pair is split into two frequencies shifted slightly upward and downward from it. While both oscillations are anti-symmetric spanwise, they are symmetric axially at the lower frequency and anti-symmetric at the higher one.

We conclude this paper with three perspectives. Pairs of Helmholtz resonators have been considered so far. If a pair of other types of cavities such as a quarter-wavelength tube is connected, analysis would parallel the present theory which assumes compact cavities to use their acoustic admittance. Then a localized mode would appear not only at a single frequency but also at multiple ones depending on the geometry of the cavity. This is seen from the graphical solution to a frequency equation corresponding to (3.13) in the case of the quarter-wavelength tube whose acoustic admittance Y is given by $\mathrm{i}B\tan(L\omega/a_0)/\rho_0 a_0$, B and L being the width and depth of the tube. Since Evans & Linton (1991), Evans *et al.* (1994) and Koch (2004) have already considered an indentation in the waveguide, the results may be compared with the existing ones. Secondly, if a circular tube with the resonators connected facing each other is considered, as in the original motivation for the present paper, it is conjectured

to be highly likely that a localized mode would appear in view of the results for a circular tube with a sphere inside by Ursell (1991). Thirdly when the identical pairs of resonators are placed periodically with equal spacing along a waveguide extending infinitely, a banded structure in the frequency appears due to Bragg reflection even in the plane-wave mode (Sugimoto & Horioka 1995). Then it is interesting to consider the existence of localized modes in the stopping bands or possibly passing bands.

The authors acknowledge the valuable comments and suggestions by three reviewers for improvement of the original manuscript.

REFERENCES

Abramian, A. K., Andreyev, V. L. & Indejtchev, D. A. 1995 Trapped modes of oscillation in an elastic system. *J. Tech. Acoust.* **2**, 3–17.

Callan, M., Linton, C. M. & Evans, D. V. 1991 Trapped modes in two-dimensional waveguides. *J. Fluid Mech.* **229**, 51–64.

Evans, D. V. 1992 Trapped acoustic modes. *IMA J. Appl. Maths* **49**, 45–60.

Evans, D. V., Levitin, M. & Vassiliev, D. 1994 Existence theorems for trapped modes. *J. Fluid Mech.* **261**, 21–31.

Evans, D. V. & Linton, C. M. 1991 Trapped modes in open channels. *J. Fluid Mech.* **225**, 153–175.

Evans, D. V., Linton, C. M. & Ursell, F. 1993 Trapped mode frequencies embedded in the continuous spectrum. *Q. J. Mech. Appl. Maths* **46**, 253–274.

Evans, D. V. & McIver, P. 1991 Trapped waves over symmetric thin bodies. *J. Fluid Mech.* **223**, 509–519.

Evans, D. V. & Porter, R. 1997 Trapped modes about multiple cylinders in a channel. *J. Fluid Mech.* **339**, 331–356.

Evans, D. V. & Porter, R. 1998 Trapped modes embedded in the continuous spectrum. *Q. J. Mech. Appl. Maths* **52**, 263–274.

Fernyhough, M. & Evans, D. V. 1998 Full multimodal analysis of an open rectangular groove waveguide. *IEEE Trans. Microwave Theory Tech.* **46**, 97–107.

Jones, D. S. 1953 The eigenvalues of $\nabla^2 u + \lambda u = 0$ when the boundary conditions are given on semi-infinite domains. *Proc. Camb. Phil. Soc.* **49**, 668–684.

Koch, W. 2004 Acoustic resonances in rectangular open cavities. *AIAA Paper* 2004-2843.

Linton, C. M. & McIver, M. 1998 Trapped modes in cylindrical waveguides. *Q. J. Mech. Appl. Maths* **51**, 389–412.

Linton, C. M., McIver, M., McIver, P., Ratcliffe, K. & Zhang, J. 2002 Trapped modes for off-centre structures in guides. *Wave Motion* **36**, 67–85.

McIver, M. & Linton, C. M. 1995 On the non-existence of trapped modes in acoustic waveguides. *Q. J. Mech. Appl. Maths* **48**, 543–555.

McIver, M., Linton, M., McIver, P., Zhang, J. & Porter, R. 2001 Embedded trapped modes for obstacles in two-dimensional waveguides. *Q. J. Mech. Appl. Maths* **54**, 273–293.

Morse, P. M. & Feshbach, H. 1953 *Methods of Theoretical Physics*, Part I. McGraw-Hill.

Noble, B. 1988 *Methods Based on the Wiener-Hopf Technique for the Solution of Partial Differential Equations.* Chelsea Publishing.

Parker, R. & Stoneman, S. A. T. 1989 The excitation and consequences of acoustic resonances in enclosed fluid flow around solid bodies. *Proc. Inst. Mech. Engrs, Part C, J. Mech. Engng Sci.* **203**, 9–19.

Porter, R. & Evans, D. V. 1999 Rayleigh-Bloch surface waves along periodic gratings and their connection with trapped modes in waveguides. *J. Fluid Mech.* **386**, 233–258.

Sugimoto, N. 1992 Propagation of nonlinear acoustic waves in a tunnel with an array of Helmholtz resonators. *J. Fluid Mech.* **244**, 55–78.

Sugimoto, N. & Horioka, T. 1995 Dispersion characteristics of sound waves in a tunnel with an array of Helmholtz resonators. *J. Acoust. Soc. Am.* **97**, 1446–1459.

Sugimoto, N., Masuda, M., Yamashita, K. & Horimoto, H. 2004 Verification of acoustic solitary waves. *J. Fluid Mech.* **504**, 271–299.

URSELL, F. 1951 Trapping modes in the theory of surface waves. *Proc. Camb. Phil. Soc.* **47**, 347–358.

URSELL, F. 1987 Mathematical aspects of trapping modes in the theory of surface waves. *J. Fluid Mech.* **183**, 421–437.

URSELL, F. 1991 Trapped modes in a circular cylindrical acoustic waveguide. *Proc. R. Soc. Lond.* A **435**, 575–589.

WOODLEY, B. M. & PEAKE, N. 1999*a* Resonant acoustic frequencies of a tandem cascade. Part 1. Zero relative motion. *J. Fluid Mech.* **393**, 215–240.

WOODLEY, B. M. & PEAKE, N. 1999*b* Resonant acoustic frequencies of a tandem cascade. Part 2. Rotating blade rows. *J. Fluid Mech.* **393**, 241–256.